

29. SULFATE REDUCTION AND RELATED STABLE ISOTOPE (^{34}S , ^{18}O) VARIATIONS IN INTERSTITIAL WATERS FROM THE EASTERN MEDITERRANEAN¹

Michael E. Böttcher,^{2,4} Hans-Jürgen Brumsack,² and Gert J. de Lange³

ABSTRACT

Interstitial waters from eleven sites of the Eastern Mediterranean Basin (Sites 963–973) were analyzed for stable isotopes of dissolved sulfate ($\delta^{34}\text{S}$, $\delta^{18}\text{O}$) and major and minor ions.

Sulfate reduction rates are positively related to bulk sedimentation rates, which indicates a higher burial of metabolizable organic matter with increasing sedimentation rates. Bacterial sulfate reduction in the deeper samples from most of the sites is superimposed by a sulfate input from Messinian evaporites or late-stage evaporite brines that are located at depth; dissolution of gypsum within the cored section was found at Sites 967 and 968. Authigenic gypsum precipitation was identified at Site 973 below 100 mbsf.

Intense sulfate reduction is also indicated for the pore waters from the mud volcanoes of Sites 970 and 971. In addition to high concentrations of hydrocarbons (mainly CH_4), coexisting H_2S and SO_4^{2-} were also present, indicating that methane percolates through the sediment from greater depths. The observed variabilities in sulfate concentrations between different holes of Sites 970 and 971 are caused mainly by locally varying-upward fluxes of methane. Extremely high alkalinity values in the pore waters of Sites 970 and 971 are the result of microbial CH_4 oxidation.

The concentration and sulfur isotopic composition of pore-water sulfate ($\delta^{34}\text{S}$ values up to +112 ‰ vs. the Vienna-Canyon Diablo troilite standard) are dominated by microbial organic matter degradation with associated sulfate reduction. Therefore, most interstitial fluids are enriched in ^{34}S with respect to modern Mediterranean seawater ($\delta^{34}\text{S} = +20.7\text{‰}$; Site 973 surface seawater). $\delta^{18}\text{O}(\text{SO}_4^{2-})$ values at Site 963 and 964 are also enriched in ^{18}O with respect to Mediterranean seawater ($\delta^{18}\text{O}[\text{SO}_4^{2-}] = +9.4\text{‰}$). $\delta^{34}\text{S}$ and $\delta^{18}\text{O}$ values of dissolved residual sulfate are positively related to each other. An initial kinetic isotope effect is superimposed by oxygen isotope exchange reactions leading to an increased equilibration between residual sulfate and pore water with increasing degree of sulfate reduction. It is suggested that $\delta^{18}\text{O}$ – $\delta^{34}\text{S}$ relations of residual sulfate directly reflect sulfate reduction rates in marine sediments.

INTRODUCTION

Sediments in the Eastern Mediterranean basin are dominated by alternating sequences of organic-poor hemipelagic sediments and organic-rich sapropels or sapropelic layers (Buckley et al., 1974; Calvert, 1983; de Lange et al., 1989), which are thought to be controlled by cyclic changes in environmental conditions (Sigl et al., 1978; Calvert, 1983; de Lange and ten Haven, 1983).

Interstitial waters from eleven sites of the Eastern Mediterranean Basin (Sites 963–973; Fig. 1) were retrieved during Leg 160 of the Ocean Drilling Program (ODP) and analyzed for stable isotopes of dissolved sulfate (^{34}S : ^{32}S , ^{18}O : ^{16}O), in addition to major and minor ions. Site 963 is in the Strait of Sicily, Site 964 is on the Pisano Plateau in the Ionian Basin, and Sites 969–973 are from the Mediterranean Ridge between the Ionian and the Levantine Basins. Sites 970 and 971 were drilled on the flanks of the now passive Milano Dome and the still active Napoli Dome mud volcanoes, respectively. Sites 965–968 are positioned on a transect between the Eratosthenes Seamount and the Cyprus margin. The recovered sediments span a time interval from the Eocene to the Holocene (Emeis, Robertson, Richter, et al., 1996). Frequent sapropel layers with organic-carbon content up to 30% by weight (Emeis, Robertson, Richter, et al., 1996) were found at almost all sites reflecting periods of enhanced organic matter production and/or preservation.

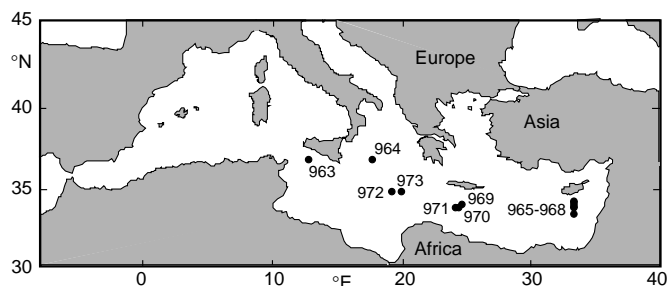


Figure 1. Outline map of the Eastern Mediterranean with sampling sites of Leg 160.

Pore waters were retrieved from all sites drilled during Leg 160 to follow the early and late diagenetic microbial organic matter degradation within the sediment column and the influence of evaporites, or late-stage evaporite brines at depth, on the interstitial waters of the overlying sediments.

SAMPLING AND ANALYTICAL METHODS

Interstitial water samples were squeezed from whole-round samples immediately after retrieval of the cores with the standard ODP titanium/stainless-steel squeezer (Manheim and Sayles, 1974) and a plastic-lined squeezer (Brumsack et al., 1992). The retrieved pore waters were subsequently analyzed on board ship for salinity, alkalinity, sulfate, chloride, bromide, lithium, potassium, rubidium, sodium, calcium, magnesium, strontium, ammonium, and silica by using the methods described in Gieskes et al. (1991). The shipboard sulfate data obtained by ion chromatography were additionally confirmed by X-ray fluorescence spectroscopy (Wehausen, pers. comm., 1996).

¹Robertson, A.H.F., Emeis, K.-C., Richter, C., and Camerlenghi, A. (Eds.), 1998. *Proc. ODP, Sci. Results*, 160: College Station, TX (Ocean Drilling Program).

²Institute of Chemistry and Biology of the Marine Environment (ICBM), Carl von Ossietzky University, P.O. Box 2503, D-26111 Oldenburg, Federal Republic of Germany.

³Department of Geochemistry, Institute of Earth Sciences, Budapestlaan 4, NL-3584 CD Utrecht, Netherlands.

⁴Present address: Department of Biogeochemistry, Max-Planck-Institute for Marine Microbiology, Celsiusstr.1, D-28359 Bremen, Federal Republic of Germany. mboettch@mpi-bremen.de

Sulfur and oxygen isotope measurements of dissolved sulfate were determined on pore waters previously used for shipboard alkalinity determinations. The sulfate was precipitated quantitatively as BaSO₄ by the addition of barium chloride, washed with deionized water, and dried at 110°C. For sulfur isotope analysis, the sulfate was converted to SO₂ via flash combustion in an elemental analyzer (Giesemann et al., 1994). Sulfur isotope ratios (³⁴S/³²S) were analyzed by combustion-isotope-ratio-monitoring mass spectrometry (C-irmMS). Since this method has not previously been described in detail, the relevant information is given in the appendix of this paper. Oxygen isotope measurements on BaSO₄ were carried out at the Marie Curie-Skolodowska University of Lublin according to the method described by Mizutani (1971). A δ¹⁸O value of +9.5‰ was obtained for the IAEA intercomparison distribute NBS-127 (BaSO₄) which agrees with the proposed value of +9.34 ± 0.32‰ (Gonfiantini et al., 1995). Stable isotope ratios ³⁴S:³²S and ¹⁸O:¹⁶O are given in the δ-notation with respect to the Vienna-Canyon-Diablo troilite (V-CDT) standard and Vienna-Standard Mean Ocean Water (V-SMOW) standards, respectively.

RESULTS AND DISCUSSION

Oxidation of Organic Matter and Methane

From the downward variation of dissolved sulfate concentrations in the interstitial waters (Figs. 2, 3), it is evident that most of the sites are characterized by more or less intense bacterial sulfate reduction. Even at those sites where the pore-water sulfate concentrations are comparable to modern Mediterranean seawater (~31 mM; surface seawater at Site 973), microbial activities using sulfate as the electron acceptor are traced by the sulfur isotopic composition of residual sulfate.

Reduction of dissolved sulfate proceeds because of the availability of metabolizable organic matter or hydrocarbons (mainly CH₄) in the sediments. Whereas sulfate reduction is essentially complete in the upper portions of cores from Holes 963A, 971B, 970C and 970D (Table 1), significant amounts of sulfate are still present in the interstitial waters of cores from all other sites. No influence of organic-rich layers (sapropels) in the sediment column was observed on the pore-water sulfate profiles.

Sulfate reduction rates (SRR) for the upper portions of the sediment sections from Sites 963, 964, 966, and 968 were calculated according to Canfield (1991) and are positively correlated to the bulk sedimentation rates (BSR; Fig. 4), which indicates higher preservation of metabolizable organic matter with an increasing sedimentation rate (Berner, 1980). The results for the Eastern Mediterranean agree well with those for the Western Mediterranean (Leg 161; Böttcher et al., in press) and a linear regression of all data yields ($r = 0.924$; $n = 9$)

$$\text{SRR [mM/(cm}^2\text{-ky)]} = -0.085 + 25.858 \cdot \text{BSR [cm/yr]}.$$

The microbial reduction of dissolved sulfate leads to a kinetic isotope effect, an enrichment of the lighter sulfur isotope ³²S in the formed hydrogen sulfide, and a corresponding rise of the isotope values of the residual sulfate (e.g. Chambers and Trudinger, 1979; Rees, 1973).

By assuming closed-system conditions with respect to dissolved sulfate (Hartmann and Nielsen, 1969; Sweeney and Kaplan, 1980), an evaluation of the residual sulfate data of Site 963 between 0 and 21.45 mbsf according to the Raleigh fractionation model yields a very good linear correlation (Fig. 5) and a fractionation factor of 1.047. This value is at the upper boundary observed experimentally for microbial sulfate reduction at low reaction rates (Chambers and Trudinger, 1979; Canfield and Teske, 1996; Rees, 1973). A contribu-

tion of sulfate diffusion from the sediment-water interface to the pore-water sulfate pool ("open system" with respect to sulfate) would increase the calculated fractionation factor (Jørgensen, 1979). It has been shown, however, that closed-system evaluation often serves as a good and internally consistent approximation for diagenetic sulfate reduction in marine systems (Hartmann and Nielsen, 1969; Sweeney and Kaplan, 1980). The sulfate profile at Site 963 shows a convex-up curvature (Fig. 2), which, together with the downward increase in alkalinity and dissolved ammonium (Fig. 6), indicates that sulfate reduction seems to be related to the microbial in situ degradation of organic matter and that upward diffusion of methane played no significant role in the upper part of the sedimentary column (Borowski et al., 1996). For the deepest pore-water sample retrieved at Site 963, a value for the residual sulfate fraction of 0.24 is calculated from the measured dissolved sulfate concentration when no additional sulfate source is considered. This extremely ³⁴S-enriched sulfate sample, however, plots significantly above the regression line obtained for samples from the upper part of the sedimentary column (Fig. 5). Based on the measured δ³⁴S value of the sample from Section 160-963A-24H-2, a theoretical residual sulfate fraction of 0.15 is calculated with the regression equation from Figure 5 when the ³⁴S:³²S fractionation factor ($\alpha = 1.047$) is taken to be constant for the whole core. Therefore, an additional source for dissolved sulfate has to be considered. A sulfate input of 18 mM from evaporites below the Site 963 core is suggested by the measured dissolved sulfate concentration and the calculated residual sulfate fraction. A corresponding increase in Sr²⁺ of about 200 µmol/L, indicates a Sr²⁺ content of the solid phase of about 134 ppm, which is only slightly below the range reported for Messinian gypsum (de Lange et al., 1990). The slight strontium deficit is probably related to some authigenic carbonate precipitation. The downcore variation of interstitial water parameters (Fig. 6) indicates that the oxidation of methane is responsible for the sulfate reduction below 130 mbsf. Therefore, microbial activities take place even in deeply buried sediments that are more than 1 Ma. The sulfur isotope value for the combined low sulfate samples between 52 and 154 mbsf is, although quite heavy (δ³⁴S = +88‰), smaller than expected from the relation given in Figure 5. This is probably due to the very low sulfate concentrations (Table 1), because somewhat smaller isotope fractionation factors are observed under sulfate-limiting conditions (Chambers and Trudinger, 1979). A minor contribution from sulfate contamination during sampling, however, cannot be completely ruled out.

Intense sulfate reduction is also indicated for the pore waters from the mud volcano Sites 970 and 971 (Fig. 3). Aside from high concentrations of hydrocarbons (mainly CH₄), coexisting H₂S and SO₄²⁻ were present (Emeis, Robertson, Richter, et al., 1996). H₂S from 3.4 mbsf at Hole 971D, for example, showed a δ³⁴S value of +27‰ vs. +47‰ for the dissolved sulfate at 1.3 mbsf (Table 1). Since methanogenesis should be separated in space from the sulfate reduction zone, it is suggested that methane percolates through the sediment from greater depth. The observed variabilities in sulfate concentrations between different holes of Sites 970 and 971 (Table 1; Fig. 3) are mainly caused by locally varying upward fluxes of methane or quantities of decomposing clathrates. Extremely high alkalinity values of up to more than 80 mM in the pore waters of Sites 970 and 971 (Emeis, Robertson, Richter, et al., 1996) result from microbial CH₄ oxidation associated with sulfate reduction. The inverse relationship between sulfate concentrations and stable isotope data in the deeper section of Hole 970A clearly shows an upward flux of a sulfate-containing brine from underlying sediments (Fig. 3).

Figure 7 summarizes all measured sulfur isotope data as a function of the residual sulfate concentration, and compares the results with some predicted general trends that are, alone or in combination, responsible for the observed variations in the interstitial waters from Site 160. It should be noted that, based on the present interstitial water results, no indication for a significant contribution of reoxidation

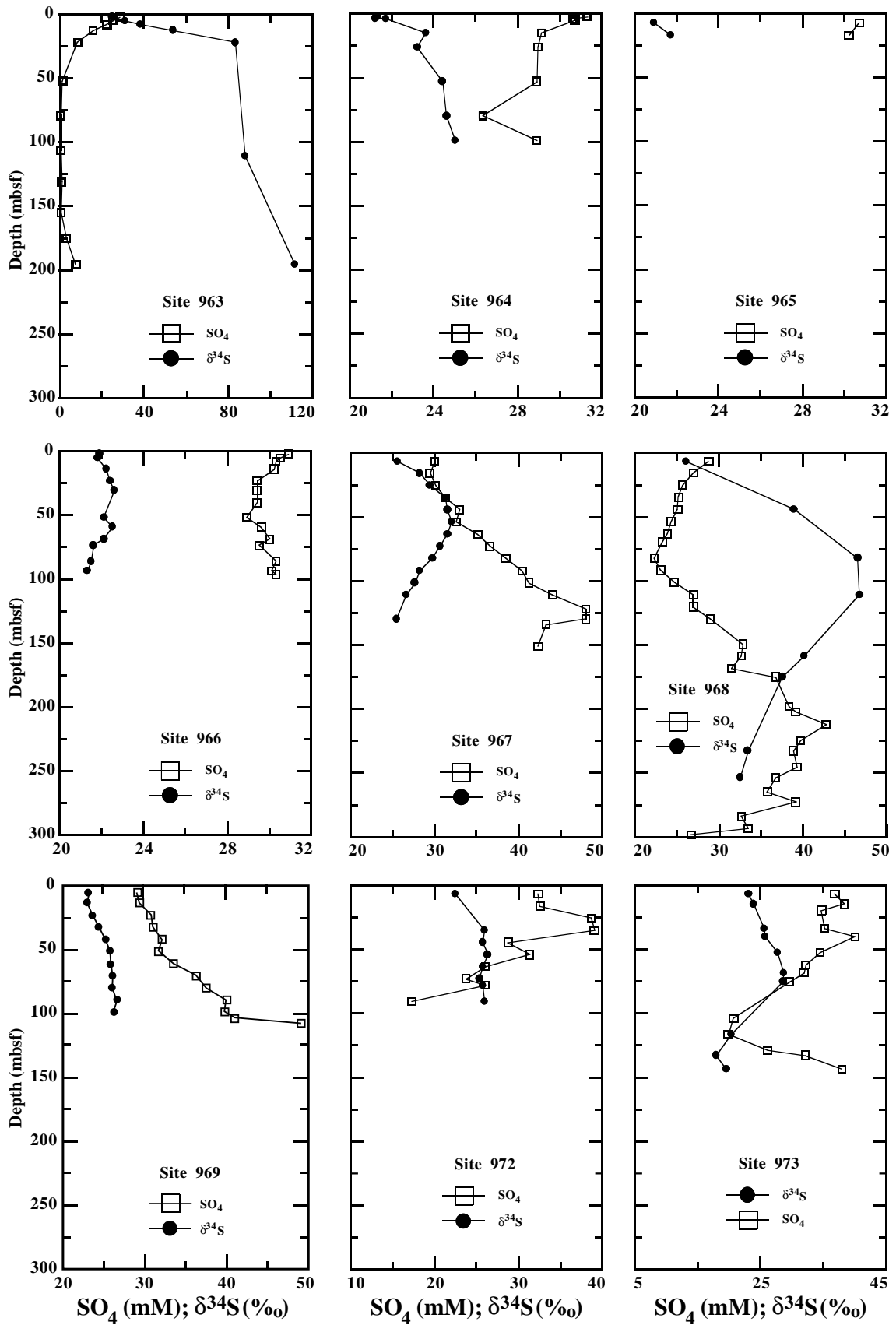


Figure 2. Pore-water sulfate concentration and δ³⁴S data vs. depth profiles of Sites 963–969, 972, and 973.

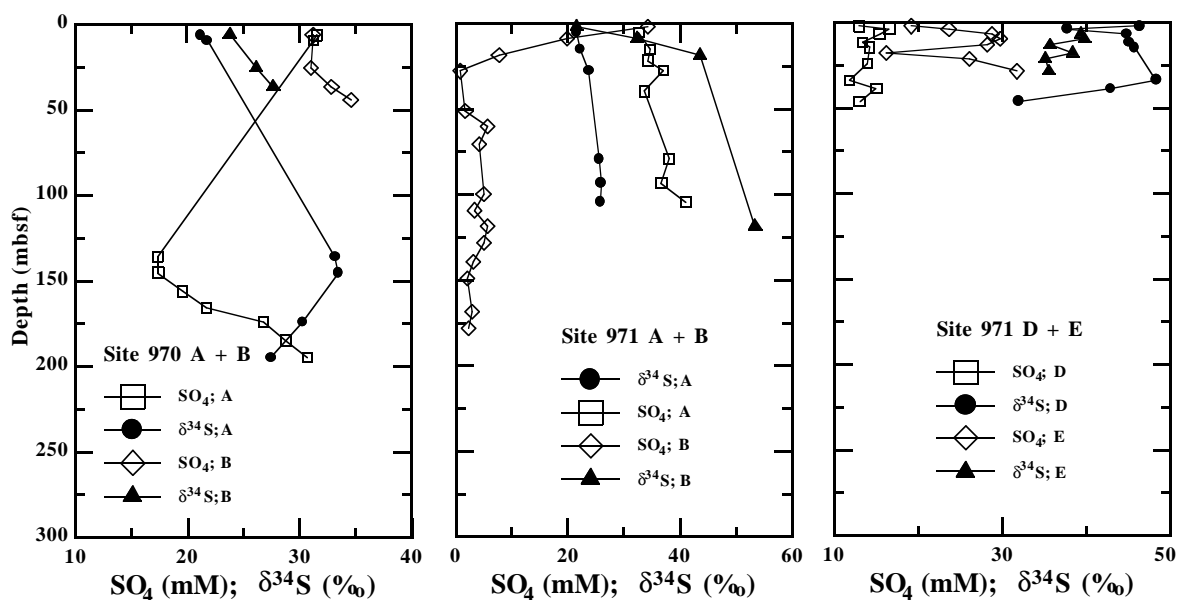


Figure 3. Pore-water sulfate concentration and $\delta^{34}\text{S}$ data vs. depth profiles of the mud volcano Sites 970 and 971.

processes involving reduced sulfur species (dissolved sulfide and/or solid sulfides) is found. Based on the geochemical results for the recent sapropels where downward migration of dissolved bisulfide into the underlying organic-poor sediments was observed (Passier et al., 1996, 1997), significant contributions from complex reoxidation and disproportionation reactions within the sulfur cycle (Canfield and Teske, 1996; Jørgensen, 1990) probably require very early diagenetic, iron-limited conditions under open-system situations with respect to oxidants and/or dissolved sulfate. As a function of time, dissolved sulfate gradients become dominated by late diagenetic unidirectional sulfate reduction processes.

The oxygen isotopic composition of residual sulfate was measured for selected interstitial waters from Sites 963 and 964 (Table 2). The dissolved sulfate was generally enriched in ^{18}O with respect to modern Mediterranean seawater sulfate ($\delta^{18}\text{O}[\text{SO}_4^{2-}] = +9.4\text{‰}$; Longinelli and Craig, 1967), and the $\delta^{18}\text{O}(\text{SO}_4^{2-})$ values increase with depth (Fig. 8). The influence of brines derived from Messinian evaporites ($\delta^{18}\text{O}[\text{SO}_4^{2-}] \approx +16\text{‰}$; Stenni and Longinelli, 1990) can be ruled out for the upper interval of Hole 963A but may have slightly influenced the deepest Site 964 sample. Although, the $\delta^{18}\text{O}(\text{SO}_4^{2-})$ values increase with increasing $\delta^{34}\text{S}$ values, the oxygen isotopic composition of the residual sulfate tends to approach a steady state (Fig. 9). For modern Eastern Mediterranean seawater, Stenni and Longinelli (1990) reported an average $\delta^{18}\text{O}(\text{H}_2\text{O})$ value of about $+1.5\text{‰}$. At 15°C , a typical water temperature in the sediment cores of Leg 160 (Emeis, Robertson, Richter, et al., 1996), the isotopic composition of dissolved sulfate in equilibrium with interstitial waters of Mediterranean seawater composition should be $+32.6\text{‰}$ when compared to the extrapolated results from hydrothermal inorganic exchange experiments (Mizutani and Rafter, 1969). The observed stable isotope data are generally below the proposed equilibrium value (Figs. 8, 9).

The inorganic oxygen isotope exchange reaction between dissolved sulfate and water at low temperatures and neutral pH is extremely slow (Chiba and Sakai, 1985; Lloyd, 1968; Mizutani and Rafter, 1969) and has been found to be negligible in oxic deep sea sediments up to 50 Ma old (Zak et al., 1980). On the other hand, significant oxygen isotope variations in dissolved sulfate have been observed in microbial sulfate reduction studies (e.g. Mizutani and Rafter, 1973; Fritz et al., 1989) and pore waters of anoxic sediments

(Zak et al., 1980). In the initial stage of sulfate reduction, kinetic isotope effects are expected to be responsible for the common increase in $\delta^{18}\text{O}$ and $\delta^{34}\text{S}$ values, because the $^{32}\text{S}-^{16}\text{O}$ bonds are weaker than the $^{34}\text{S}-^{16}\text{O}$ and $^{32}\text{S}-^{18}\text{O}$ bonds (Zak et al., 1980). For the ratio of the kinetic enrichment factors $\epsilon_{18\text{O}}/\epsilon_{34\text{S}}$ typical values between about 0.2 and 0.4 are reported (Fritz et al., 1989). From the data in Tables 1 and 2, however, highly variable $\epsilon_{18\text{O}}/\epsilon_{34\text{S}}$ values between 0.5 and 1.5 (Site 963) and between 0.3 and 1.3 (Site 964) are calculated. Similar results are observed in other anoxic sediments (Zak et al., 1980). From Figure 5 it is evident that the variation of $\delta^{18}\text{O}(\text{SO}_4^{2-})$ values as a function of $\ln F$ does not fall on a linear trend as expected for unidirectional kinetic isotope fractionation. This difference is caused by a superimposition of the kinetic isotope effect by oxygen isotope exchange reactions with the aqueous solution. This leads to an increased equilibration between residual sulfate and pore water with an increasing degree of microbial sulfate reduction. A sulfate-enzyme complex that is formed as an intermediate reaction product during dissimilatory sulfate reduction by bacteria is supposed to facilitate the observed isotope exchange with water until equilibration (Fritz et al., 1989). Figure 9 shows that the oxygen isotopes equilibrate more rapidly than the $\delta^{34}\text{S}$ values increase at Site 964 when compared to Site 963. This is caused by a lower SRR at Site 964 (Fig. 4) which enables a more intense oxygen isotope exchange upon reaction even at low degrees of sulfate reduction. This is additionally confirmed by a comparison with the results from a sediment with a high BSR and SRR from the San Pedro Martir basin in the Gulf of California (Fig. 9). The distinct relationships between $\delta^{18}\text{O}$ and $\delta^{34}\text{S}$ values seem to be related to their different sulfate reduction rates. It is therefore suggested that different sulfate reduction rates in marine sediments are directly reflected on the $\delta^{18}\text{O}-\delta^{34}\text{S}$ plots.

Effect of Evaporites, Brines, and the Formation of Authigenic Gypsum and Baryte

For most sites, an increase in sulfate concentration is found deeper downcore (Figs. 2 and 3). This is due to a superimposition of bacterial sulfate reduction by sulfate input from Messinian evaporites or late-stage evaporite brines that are located at depth. The upward sulfate flux from saline brines located at depth is inferred from salinity and major element variations of the interstitial waters from Sites 969,

Table 1. Stable sulfur isotopes in pore waters from Leg 160.

Core, section, interval (cm)	Depth (mbsf)	SO ₄ (mM)	δ ³⁴ S (‰)	Core, section, interval (cm)	Depth (mbsf)	SO ₄ (mM)	δ ³⁴ S (‰)	Core, section, interval (cm)	Depth (mbsf)	SO ₄ (mM)	δ ³⁴ S (‰)
160-963A-				5H-4, 145-150	43.45	25.0	+38.9	4H-3, 135-150	26.85	36.9	+23.6
2H-5, 145-150	11.95	15.6	+53.5	6H-4, 145-150	52.95	24.2	—	6X-1, 56-71	38.76	33.5	—
3H-5, 145-150	21.45	8.2	+83.0	7H-4, 145-150	62.45	23.8	—	10X-1, 135-150	78.35	37.9	+25.5
6H-5, 145-150	51.45	0.9	—	8H-4, 145-150	68.95	23.2	—	11X-4, 135-150	92.55	36.5	+25.8
9H-5, 145-150	78.45	0.25	—	9H-4, 145-150	81.45	22.2	+46.5	12X-5, 135-150	103.65	40.9	+25.7
12H-5, 140-150	106.0	0.3	+87.7*	10X-4, 140-150	90.95	23.0	—				
15H-4, 140-150	130.5	0.6	—	11X-4, 140-150	100.45	24.6	—	160-971B-			
18H-2, 140-150	154.4	0.35	—	12X-4, 140-150	110.0	26.9	+46.7	1H-1, 104-109	1.04	34.2	+21.4
21H-3, 140-150	174.8	2.8	—	13X-4, 140-150	119.6	26.9	—	2H-4, 140-150	8.1	19.7	+32.2
24H-2, 140-150	194.9	7.3	+111.5	14X-4, 140-150	129.2	28.9	—	3H-4, 140-150	17.6	7.58	+43.5
160-963D-				16X-4, 140-150	148.8	32.8	—	4H-5, 135-150	27.05	0.74	—
1H-1, 145-150	1.45	28.4	+24.7	17X-4, 140-150	158.1	32.6	+40.1	7X-1, 115-135	50.45	1.63	—
1H-3, 145-150	4.45	25.1	+30.9	18X-4, 140-150	167.7	31.4	—	8X-1, 61-81	59.51	5.61	—
1H-5, 145-150	7.45	22.1	+38.2	19X-2, 140-150	174.4	36.7	+37.5	9X-CC, 0-10	69.75	4.14	—
160-964A-				23X-1, 150-155	197.5	38.3	—	12X-2, 0-20	98.88	4.83	—
2H-5, 145-150	14.25	29.1	+23.6	24X-1, 140-150	201.8	39.1	—	13X-1, 130-150	108.4	3.2	—
3H-6, 145-150	25.25	29.0	+23.2	25X-1, 140-150	211.5	42.7	—	14X-1, 130-150	118.0	5.47	+53.3
6H-5, 145-150	52.25	28.9	+24.4	26X-3, 140-150	224.1	39.7	—	15X-1, 96-114	127.26	4.91	—
9H-4, 140-150	79.2	26.3	+24.6	27X-2, 130-150	232.1	38.8	+33.4	16X-2, 124-144	138.74	2.95	—
11H-4, 140-150	98.2	28.9	+25.0	28X-4, 140-150	244.8	39.2	—	17X-3, 0-20	148.53	1.96	—
160-964F-				29X-3, 140-150	253.0	36.7	+32.5	19X-2, 130-150	167.7	2.73	—
1H-1, 145-150	1.45	31.3	+21.3	30X-4, 140-150	264.1	35.7	—	20X-3, 0-26	177.4	2.19	—
1H-2, 145-150	2.95	30.6	+21.2	31X-3, 140-150	272.2	39.1	—	160-971D-			
1H-3, 145-150	4.45	30.7	+21.7	32X-4, 140-150	283.3	32.6	—	1H-1, 135-150	1.35	12.9	+46.2
160-965A-				33X-4, 140-150	292.95	33.4	—	1H-2, 135-150	2.85	16.5	+37.6
2H-4, 145-150	6.75	30.7	+20.9	34X-1, 112-127	297.72	26.6	—	1H-4, 135-150	5.85	15.3	+44.7
3H-4, 145-150	16.25	30.2	+21.7	160-969A-				2H-2, 135-150	10.85	13.3	+45.0
160-966A-				1H-4, 145-150	5.95	29.3	+23.3	2H-4, 135-150	13.85	14.1	+45.6
2H-5, 145-150	13.25	30.2	+22.2	2H-4, 145-150	13.65	29.5	+23.1	3H-4, 135-150	23.35	13.8	—
3H-5, 145-150	22.75	29.4	+22.4	3H-4, 140-150	23.1	30.9	+23.7	4H-4, 135-150	32.85	11.7	+48.2
6H-5, 145-150	51.25	28.9	+22.1	4H-4, 140-150	32.6	31.1	+24.5	5H-1, 135-150	37.85	14.9	+42.8
160-966D-				5H-4, 140-150	42.1	32.3	+25.4	5H-6, 135-150	45.35	13.0	+31.8
4H-5, 145-150	29.95	29.4	+22.6	6H-4, 140-150	51.34	31.8	+25.9	160-971E-			
5H-5, 145-150	39.45	29.4	—	7H-4, 140-150	61.1	33.6	+26.0	1H-1, 140-150	1.4	19.1	—
7H-5, 145-150	58.45	29.6	+22.5	8H-4, 140-150	70.6	36.3	+26.2	1H-2, 140-150	2.9	23.5	—
8H-5, 145-150	67.95	30.0	+22.1	9H-4, 140-150	80.1	37.6	+26.1	1H-4, 140-150	5.9	28.7	+39.3
9H-2, 145-150	72.95	29.5	+21.6	10H-4, 140-150	89.6	40.1	+26.8	1H-6, 140-150	8.9	29.6	+39.7
10H-4, 145-150	85.45	30.3	+21.5	11H-4, 140-150	99.1	39.8	+26.3	2H-2, 140-150	12.4	28.1	+35.6
12H-3, 140-150	92.9	30.1	+21.3	12H-2, 73-80	103.68	41.0	—	2H-5, 130-140	16.8	16.1	+38.3
13H-cc, 140-150	95.78	30.3	—	13H-2, 70-75	107.7	49.2	—	3H-1, 135-150	20.35	26.0	+35.0
160-966E-				160-970A-				3H-7, 69-84	27.81	31.6	+35.4
1H-1, 145-150	1.45	30.9	+21.9	1H-4, 140-150	5.9	31.5	+21.1	160-972A-			
1H-3, 145-150	4.45	30.5	+21.8	2H-1, 135-150	8.95	31.2	+21.7	1H-4, 145-150	5.95	32.3	+22.4
1H-5, 145-150	7.45	30.3	—	16X-1, 135-150	135.35	17.3	+33.1	2H-4, 145-150	15.45	32.5	—
160-967A-				17X-1, 135-150	144.95	17.3	+33.4	3H-4, 110-120	24.6	38.6	—
1H-4, 145-150	5.95	30.0	+25.5	18X-2, 135-150	155.85	19.5	—	4H-4, 140-150	34.4	39.0	+25.9
2H-4, 145-150	15.25	29.4	+28.2	19X-2, 123-138	165.53	21.7	—	5H-4, 140-150	43.9	28.7	+25.7
3H-4, 145-150	24.75	30.1	+29.4	20X-1, 135-150	173.85	26.7	+30.2	6H-4, 140-150	53.4	31.3	+26.3
4H-4, 145-150	34.25	31.2	+31.2	21X-2, 95-115	184.55	28.7	—	7H-4, 140-150	62.9	26.0	+25.7
5H-4, 145-150	43.75	32.9	+31.5	22X-2, 130-150	194.5	30.6	+27.4	8X-4, 140-150	72.4	23.7	+25.3
6H-4, 145-150	53.25	32.5	+32.0	160-970B-				9X-1, 135-150	77.45	26.0	+25.7
7H-4, 145-150	62.75	35.1	+31.5	1H-4, 140-150	5.9	31.1	+23.7	10X-3, 135-150	90.05	17.2	+25.9
8H-4, 145-150	72.25	36.5	+30.6	3H-4, 140-150	24.9	31.0	+26.1	160-973A-			
9H-4, 145-150	81.75	38.4	+29.7	4H-5, 140-150	35.9	32.8	+27.6	1H-4, 140-150	5.9	36.7	+23.0
10H-4, 145-150	91.25	40.4	+28.2	5H-4, 140-150	43.63	34.5	—	2H-4, 140-150	13.9	38.2	+23.8
11H-4, 145-150	100.75	41.2	+27.6	160-970C-				3H-1, 140-150	18.9	34.6	—
12H-4, 140-150	110.20	44.0	+26.6	1H-2, 145-150	2.95	0.66	—	4H-4, 140-150	32.9	35.1	+25.5
13H-5, 140-150	121.20	48.0	—	2H-2, 132-142	7.52	0.54	—	5H-2, 140-150	39.4	39.9	+25.6
14X-4, 140-150	129.20	48.0	+25.4	3H-2, 0-10	9.7	0.58	—	6H-4, 140-150	51.9	34.4	+27.6
15X-3, 140-150	133.50	43.2	—	160-970D-				7H-4, 140-150	61.4	32.1	—
160-967E-				1H-1, 127-150	1.27	0.8	—	8X-2, 140-150	67.9	31.8	+28.6
5R-2, 86-99	150.36	42.3	—	2H-5, 130-150	12.1	0.2	—	9X-1, 0-10	74.5	29.6	+28.5
160-968A-				3H-6, 130-150	23.1	0.3	—	12X-CC, 0-1	103.3	20.6	—
1H-4, 145-150	5.95	28.7	+26.0	4H-5, 130-150	30.71	0.1	—	13X-2, 135-150	115.75	19.8	+20.3
2H-4, 145-150	14.95	26.9	—	5H-6, 130-150	41.8	0.5	—	14X-4, 130-150	128.3	26.0	—
3H-4, 145-150	24.45	25.6	—	160-971A-				15X-1, 0-10	132.1	32.0	+17.9
4H-4, 145-150	33.95	25.1	—	1H-3, 140-150	4.4	32.6	+21.4	16X-1, 113-123	142.83	37.8	+19.5
				2H-5, 140-150	14.4	34.5	+22.1				
				3H-3, 140-150	20.9	34.1	—				

Notes: * = composite value for Sections 160-963A-6H-5 through 18H-2. — = not determined.

971, 972, and 973, and Hole 970B (Emeis, Robertson, Richter, et al., 1996). On the other hand, low salinity waters at the mud volcano Site 970 are presumably caused by the decomposition of methane clathrates upon sampling. At Site 963, the sulfate input from evaporites is not associated with an increase in salinity. It is, however, clearly seen in the increase of dissolved sulfate below about 160 mbsf and the isotopically extremely heavy residual sulfate at 195 mbsf (Table 1).

The deeper samples from Sites 963, 966–969 and 973 indicate input of sulfate from Messinian evaporites located at depth with a δ³⁴S

value around +23‰ (Stenni and Longinelli, 1990; de Lange et al., 1990; Böttcher et al., in press). Because the dissolution of sulfate minerals from evaporites does not lead to sulfur isotope fractionation (Böttcher and Uzdowski, 1993), Messinian sulfates must contribute to the sulfur isotopic composition of the interstitial sulfate with δ³⁴S values of about +23‰, which is in general agreement with the observed variation of δ³⁴S values (Fig. 2).

At Sites 967 (below ~110 mbsf) and 968 (below ~180 mbsf) gypsum was found in the sediment cores; the pore-water profiles give

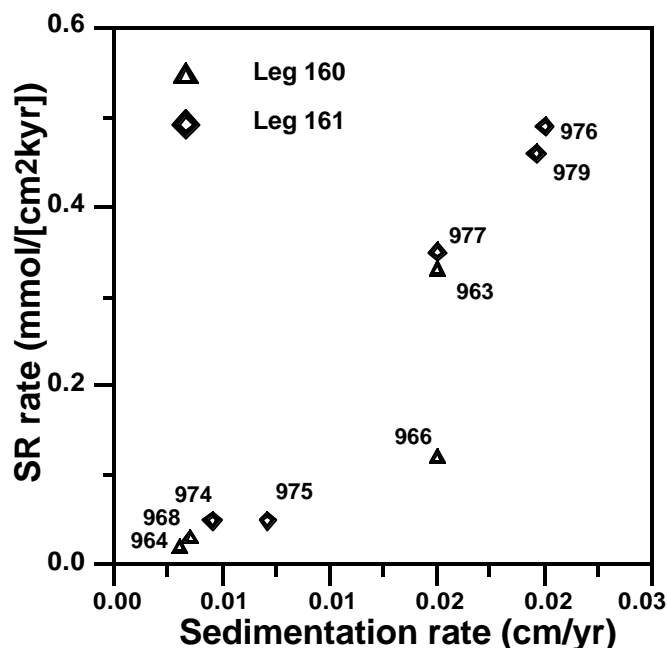


Figure 4. Variation of sulfate reduction rates of selected sites from the Eastern (Leg 160; this study) and the Western Mediterranean (Leg 161; Böttcher et al., in press) as a function of the sedimentation rate (SR).

clear evidence for the local dissolution of calcium sulfates until saturation with gypsum was attained (Fig. 2; Emeis, Robertson, Richter, et al., 1996).

Authigenic gypsum precipitation in small veins was found at Site 973 below about 110 mbsf (Emeis, Robertson, Richter, et al., 1996), which is in agreement with a minimum in the sulfate concentration profile (Fig. 2). The sulfur isotopic composition of authigenic gypsum recovered from the site ($\delta^{34}\text{S} \approx +21.5\%$; Table 3) is distinct from that of Messinian evaporites, which have a $\delta^{34}\text{S}$ value around +23‰ (Stenni and Longinelli, 1990; de Lange et al., 1990; Böttcher et al., in press). Considering an enrichment of $\delta^{34}\text{S}$ by about +1.6‰ in the solid during crystallization of gypsum (Thode and Monster, 1965), the mother solution of the Site 973 gypsum should have had an isotopic composition around +20‰, similar to the interstitial waters retrieved from the sediments below 120 mbsf (Table 1; Fig. 2). The slight depletion of these pore waters in ^{34}S with respect to modern Mediterranean seawater may be caused by a “reservoir effect” during gypsum precipitation (Fig. 7).

High barium concentrations (Ba^{2+} up to 74 μM) are observed at Site 963 where sulfate is low (Böttcher et al., 1996), reflecting dissolution of biogenic barite following sulfate reduction. From the variation of pore-water concentrations of sulfate and Ba^{2+} , the development of two “barite fronts” (Brumsack, 1986; Brumsack et al., 1992; Torres et al., 1996) at Site 963 is expected at 30–40 mbsf and 130–140 mbsf (Fig. 2). The diagenetic barite should be extremely enriched in ^{34}S with respect to modern Mediterranean surface water, based on the isotopic composition of dissolved sulfate (around +80‰ vs. V-CDT).

CONCLUSIONS

The variation of concentration and stable isotopic compositions ($\delta^{34}\text{S}$, $\delta^{18}\text{O}$) of interstitial water sulfate from the Eastern Mediterranean is dominated by the following processes:

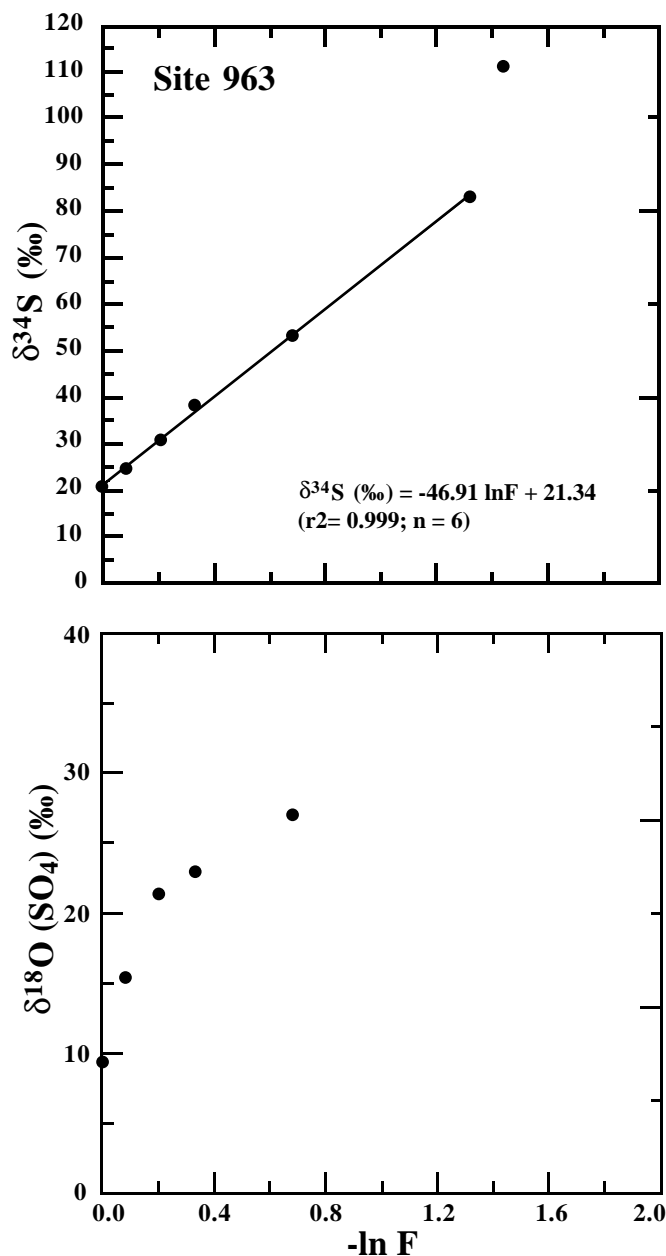


Figure 5. $\delta^{34}\text{S}$ and $\delta^{18}\text{O}$ values of residual sulfate of Site 963 as a function of the natural logarithm of the residual sulfate fraction F.

1. Microbiological degradation of organic matter and related sulfate reduction in the upper sediment column;
2. Bacterial oxidation of methane and related sulfate reduction at the mud volcano sites (Sites 970 and 971) and at least the deeper part of Site 963;
3. Dissolution of gypsum (Sites 967 and 968);
4. Dissolved sulfate derived from Messinian evaporites or late-stage evaporite brines located at depth; and
5. Precipitation of authigenic gypsum at Site 973.

Sulfur and oxygen isotope measurements on the dissolved sulfate of interstitial waters from the Eastern Mediterranean are shown to be a powerful tool in the evaluation of sinks, sources, and microbiological transformation reactions upon diagenesis of the sediments. It is

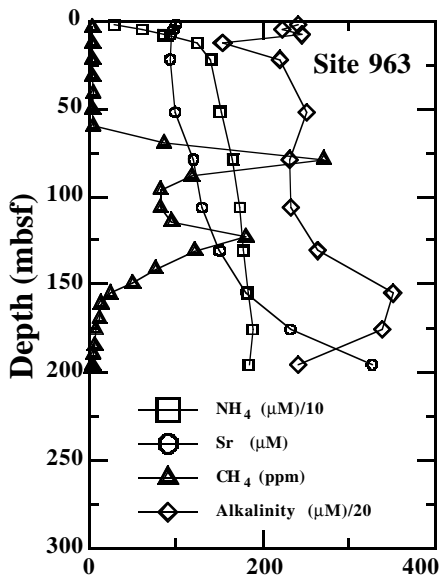


Figure 6. Downhole variations of ammonium, strontium, methane, and alkalinity concentrations from Site 963 (data from Emeis, Robertson, Richter, et al., 1996).

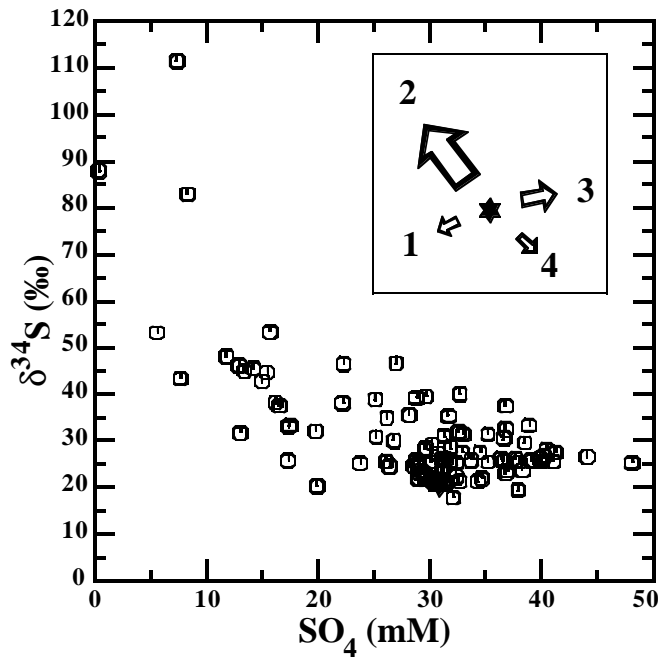


Figure 7. $\delta^{34}\text{S}$ vs. concentration of residual sulfate of all measured pore waters from Site 160 and a schematic diagram showing how different processes may influence the composition of dissolved sulfate. Arrows = theoretical trends starting with Mediterranean seawater (star; surface water at Site 973) with numbers designated as follows: 1 = authigenic precipitation of gypsum; 2 = microbial sulfate reduction; 3 = dissolution of Messinian gypsum; and 4 = reoxidation of dissolved sulfide. Note that the direction of the gypsum dissolution arrow may change when other initial values for the solution are considered. Arrow sizes = the estimated overall importance for the Leg 160 pore waters.

Table 2. Stable oxygen isotopes in pore-water sulfates from Leg 160.

Core, section	$\delta^{18}\text{O}$ (‰)
160-963A-2H-5	+27.1
160-963D-1H-1	+15.5
160-963D-1H-3	+21.4
160-963D-1H-5	+22.9
160-964A-2H-5	+21.3
160-964A-3H-6	+20.1
160-964A-6H-5	+22.0
160-964A-11H-4	+22.3
160-964F-1H-1	+11.0
160-964F-1H-3	+14.9

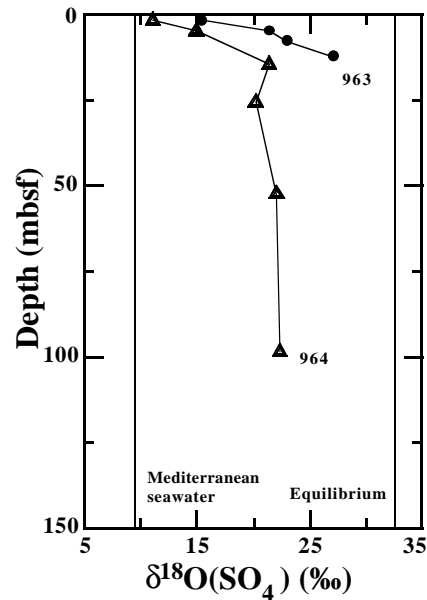


Figure 8. Downhole variations of $\delta^{18}\text{O}$ of the residual sulfate at Sites 963 and 964.

Table 3. Stable sulfur isotopes of authigenic gypsum from Site 973.

Core, section interval (cm)	$\delta^{34}\text{S}$ (‰)
160-973A-13X-2, 140-150	+21.7
160-973D-8X-1	+21.1

additionally suggested that different sulfate reduction rates in marine sediments are directly reflected by $\delta^{18}\text{O}$ – $\delta^{34}\text{S}$ plots.

ACKNOWLEDGEMENTS

We thank the scientific and technical crew of Leg 160 for support during sampling. We further acknowledge the oxygen isotope measurements by J. Szaran and S. Halas, and the supply of a synthetic CdS standard by A. Giesemann. Musical inspiration by the United Jazz + Rock Ensemble during manuscript preparation was highly appreciated. The final manuscript benefited from the reviews of A. Aplin, M. Kersten, and M.E. Torres. This study was funded by the German Science Foundation (DFG) during ODP SPP.

REFERENCES

- Berner, R.A., 1980. *Early Diagenesis: A Theoretical Approach*: Princeton, NJ (Princeton Univ. Press).
- Borowski, W.S., Paull, C.K., and Ussler, W., III, 1996. Marine pore water sulfate profiles indicate in situ methane flux from underlying gas hydrate. *Geology*, 24:655–658.
- Böttcher, M.E., Bernasconi, S.M., and Brumsack, H.-J., in press. Carbon, sulfur and oxygen isotope geochemistry of interstitial waters from Leg 161. In Zahn, R., Comas, M.C., Klaus, A., and Cita-Sironi, M.-B. (Eds.), *Proc. ODP, Sci. Results*, 161: College Station, TX (Ocean Drilling Program).
- Böttcher, M.E., Brumsack, H.-J., de Lange, G.J., Schnetger, B., and Leg 160 Scientific Party, 1996. Sulfate reduction, and related element and stable isotope variations in pore waters of sediments from the Eastern Mediterranean basin (Leg 160). *Terra Nostra*, 96:25–26.
- Böttcher, M.E., and Uzdowski, E., 1993. $34S/32S$ ratios of the dissolved sulphate of river, well and spring waters in a gypsum-carbonate karst area at the southwest edge of the Harz mountains. *Z. Dtsch. Geol. Ges.*, 144:471–477.
- Brumsack, H.-J., 1986. The inorganic geochemistry of Cretaceous black shales (DSDP Leg 41) in comparison to modern upwelling sediments from the Gulf of California. In Summerhayes, C.P., and Shackleton, N.J. (Eds.), *North Atlantic Palaeoceanography*. Geol. Soc. London Spec. Publ., 21:447–462.
- Brumsack, H.-J., Zuleger, E., Gohn, E., and Murray, R.W., 1992. Stable and radiogenic isotopes in pore waters from Leg 127, Japan Sea. In Pisciotto, K.A., Ingle, J.C., Jr., von Breyman, M.T., Barron, J., et al., *Proc. ODP, Sci. Results*, 127/128 (Pt. 1): College Station, TX (Ocean Drilling Program), 635–650.
- Buckley, H.A., Easton, A.J., and Johnson, L.R., 1974. Iron and manganese encrustations in recent sediments. *Nature*, 249:436–437.
- Calvert, S.E., 1983. Geochemistry of Pleistocene sapropels and associated sediments from the Eastern Mediterranean. *Oceanol. Acta*, 6:225–267.
- Canfield, D.E., 1991. Sulfate reduction in deep-sea sediments. *Am. J. Sci.*, 291:177–188.
- Canfield, D.E., and Teske, A., 1996. Late Proterozoic rise in atmospheric oxygen concentration inferred from phylogenetic and sulfur-isotope studies. *Nature*, 328:127–132.
- Chambers, L.A., and Trudinger, P.A., 1979. Microbiological fractionation of stable sulfur isotopes: a review and critique. *Geomicrobiol. J.*, 1:249–293.
- Chiba, H., and Sakai, H., 1985. Oxygen isotope exchange rate between dissolved sulfate and water at hydrothermal temperatures. *Geochim. Cosmochim. Acta*, 49:993–1000.
- Crusius, J., Calvert, S., Pedersen, T., and Sage, D., 1996. Rhenium and molybdenum enrichments in sediments as indicators of oxic, suboxic and sulfidic conditions of deposition. *Earth Planet. Sci. Lett.*, 145:65–78.
- de Lange, G.J., Bielrijk, N.A.I.M., Catalano, G., Corselli, C., Klinkhammer, G.P., Middelburg, J.J., Muller, D.W., Ullmann, W.J., Van Gaans, P., and Woittiez, J.R.W., 1990. Sulphate-related equilibria in the hypersaline brines of the Tyro and Bannock Basins, Eastern Mediterranean. *Mar. Chem.*, 31: 89–112.
- de Lange, G.J., Middelburg, J.J., and Pruyssers, P.A., 1989. Discussion: Middle and Late Quaternary depositional sequences and cycles in the Eastern Mediterranean. *Sedimentology*, 36:151–158.
- de Lange, G.J., and ten Haven, H.L., 1983. Recent sapropel formation in the Eastern Mediterranean. *Nature*, 305:797–798.
- Emeis, K.-C., Robertson, A.H.F., Richter, C., et al., 1996. *Proc. ODP, Init. Repts.*, 160: College Station, TX (Ocean Drilling Program).
- Fritz, P., Basharmal, G.M., Drimmie, R.J., Ibsen, J., and Qureshi, R.M., 1989. Oxygen isotope exchange between sulphate and water during bacterial reduction of sulphate. *Chem. Geol. (Isot. Geosc. Sec.)*, 79:99–105.
- Giesemann, A., Jäger, H.-J., Norman, A.L., Krouse, H.R., and Brand, W.A., 1994. On-line sulphur isotope determination using an elemental analyzer coupled to a mass spectrometer. *Anal. Chem.*, 66:2816–2819.
- Gieskes, J.M., Gamo, T., and Brumsack, H., 1991. Chemical methods for interstitial water analysis aboard *JOIDES Resolution*. *ODP Tech. Note*, 15.
- Gonfiantini, R., Stichler, W., and Rozanski, K., 1995. Standards and inter-comparison materials distributed by the International Atomic Energy Agency for stable isotope measurements. IAEA-TECDOC-825, 13–29.
- Hartmann, M., and Nielsen, H., 1969. $d34S$ -Werte in rezenten Meeressedimenten und ihre Deutung am Beispiel einiger Sedimentprofile aus der westlichen Ostsee. *Geol. Rundsch.*, 58:621–655.
- Jørgensen, B.B., 1979. A theoretical model of the stable sulfur isotope distribution in marine sediments. *Geochim. Cosmochim. Acta*, 31:363–374.
- , 1990. A thiosulfate shunt in the sulfur cycle of marine sediments. *Science*, 249:152–154.
- Lloyd, R.M., 1968. Oxygen isotope behavior in the sulfate-water system. *J. Geophys. Res.*, 73:6099–6110.
- Longinelli, A., and Craig, H., 1967. Oxygen-18 variations in sulfate ions in sea-water and saline lakes. *Science*, 146:56–59.
- Manheim, F.T., and Sayles, F.L., 1974. Composition and origin of interstitial waters of marine sediments, based on deep sea drill cores. In Goldberg, E.D. (Ed.), *The Sea (Vol. 5): Marine Chemistry: The Sedimentary Cycle*: New York (Wiley), 527–568.
- Mizutani, Y., 1971. An improvement of the carbon-reduction method for the oxygen isotopic analysis of sulphates. *Geochem. J.*, 5:69–77.
- Mizutani, Y., and Rafter, T.A., 1969. Oxygen isotopic composition of sulphates?part 3: Oxygen isotopic fractionation in the bisulphate ion-water system. *N.Z. J. Sci.*, 12:54–59.
- , 1973. Isotopic behaviour of sulphate oxygen in the bacterial reduction of sulphate. *Geochem. J.*, 6:183–191.
- Passier, H.F., Middelburg, J.J., de Lange, G.J., and Böttcher, M.E., 1997. Pyrite contents, microtextures and sulphur isotopes in relation to formation of the youngest Eastern Mediterranean sapropel. *Geology*, 25:519–522.
- Passier, H.F., Middelburg, J.J., Van Os, B.J.H., and de Lange, G.J., 1996. Diagenetic pyritization under Eastern Mediterranean sapropels caused by downward sulphide diffusion. *Geochim. Cosmochim. Acta*, 60:751–763.
- Rees, C.E., 1973. A steady state model for sulfur isotope fractionation in bacterial reduction processes. *Geochim. Cosmochim. Acta*, 37:1141–1162.
- Sigl, W., Chamley, H., Fabricius, F., Giroud d'Argoud, G., and Mueller, J., 1978. Sedimentology and environmental conditions of sapropels. In Hsü, K.J., Montadert, L., et al., *Init. Repts. DSDP*, 42: Washington (U.S. Govt. Printing Office), 445–465.
- Stenni, B., and Longinelli, A., 1990. Stable isotope study of water, gypsum and carbonate samples from the Bannock and Tyro Basins, Eastern Mediterranean. *Mar. Chem.*, 31:123–135.
- Sweeney, R.E., and Kaplan, I.R., 1980. Diagenetic sulfate reduction in marine sediments. *Mar. Chem.*, 21:165–174.
- Thode, H.G., and Monster, J., 1965. Sulfur isotope geochemistry of petroleum, evaporites and ancient seas. In *Fluids in Subsurface Environments*. AAPG Mem., 4:367–377.
- Torres, M.E., Brumsack, H.-J., Bohrmann, G., and Emeis, K.C., 1996. Barite fronts in continental margin sediments: a new look at barium remobilization in the zone of sulfate reduction and formation of heavy barites in diagenetic fronts. *Chem. Geol.*, 127:125–139.
- Zak, I., Sakai, H., and Kaplan, I.R., 1980. Factors controlling the $^{18}O/^{16}O$ and $^{34}S/^{32}S$ isotope ratios of ocean sulfates, evaporites and interstitial sulfates from modern deep sea sediments. In Goldberg, E.D., Horibe, Y., and Saruhashi, K. (Eds.), *Isotope Marine Chemistry*: Tokyo (Rokakuho), 339–373.

Date of initial receipt: 17 January 1997

Date of acceptance: 22 June 1997

Ms 160SR-002

APPENDIX

$^{34}\text{S}/^{32}\text{S}$ ratios of BaSO_4 were measured by means of combustion isotope-ratio-monitoring mass spectrometry (C-irmMS) using a Carlo Erba EA 1108 elemental analyzer connected to a Finnigan MAT 252 mass spectrometer via a Finnigan MAT Conflo II split interface. About 0.5 mg BaSO_4 were wrapped together with about 0.2 mg V_2O_5 (Carlo Erba or Hekatech) in Sn capsules (Hekatech; 4 x 6 mm). The caps were introduced into the reaction tube of the elemental analyzer via an autosampler (Carlo Erba), which was permanently flushed with helium (5.0 grade). They were combusted in a pulse of oxygen (grade 4.6, Messer Griesheim) at 1100°C. Flash combustion resulted from the exothermic oxidation of Sn to SnO, yielding a short increase of temperature to about 1800°C. The liberated sample gas (SO_2 with traces of SO_3) was transported in a continuous stream of highly pure helium (5.0 grade; 80 ml/min flow rate). SO_3 was reduced to SO_2 over highly pure reduced Cu (Hekatech) in the reduction zone of the reaction tube at 1100°C. Water was removed from the gas stream by a water trap filled with magnesium perchlorate, and SO_2 was separated from other gas impurities by a chromatographic column (0.8 m length; PTFE tubing) at 80°C. A split of the total gas stream was introduced into the gas mass spectrometer via a fused silica capillary using a Finnigan MAT Conflo II interface, and the ion currents of masses 66 and 64 in the sam-

ple gas were compared to the corresponding ion currents of external in-house BaSO_4 standards that were combusted every 15–20 samples. Comparison was done via a commercial SO_2 gas (Messer Griesheim, 4.6 grade; $\delta^{66}\text{S}$ near V-CDT composition), which was introduced into the mass spectrometer (for 20 s) before the respective sample gas pulse from the elemental analyzer arrived. A pressure of about 10^{-6} mbar was maintained in the mass spectrometer system by differential pumping. The ion currents were recorded as a function of time, and the areas underneath the peaks for masses 64 and 66 were intergrated using integration time steps of 0.25 s. Data evaluation was carried out with the Finnigan MAT Isodat 5.2 software. Replicate analyses agreed within $\pm 0.2\%$. IAEA-S-1 ($\delta^{34}\text{S} = -0.30\%$; Ag_2S), and IAEA-S-2 ($\delta^{34}\text{S} = +21.54\%$; Ag_2S) were used for calibration of the mass spectrometer. $\delta^{34}\text{S}$ values of $+20.59 \pm 0.08\%$ ($n = 10$), $+17.29 \pm 0.26\%$ ($n = 9$), $-32.29 \pm 0.13\%$ ($n = 2$) and $+16.34 \pm 0.10\%$ ($n = 2$) were obtained for IAEA intercomparison distributes NBS-127 (BaSO_4), NBS-123 (ZnS), IAEA-S-3 (Ag_2S) and IAEA-S-4 (elemental S), respectively. $\delta^{34}\text{S} = 11.0 \pm 0.1\%$ ($n = 10$) was measured for a synthetic CdS standard supplied by A. Giesemann (FAL Braunschweig). The isotopic compositions of the standards were determined directly as described above without further chemical pretreatments. The measured values compare very well to the presently accepted data (Fig. 10; Gröning (IAEA Vienna), pers. comm., 1995; Giesemann, pers. comm., 1995).

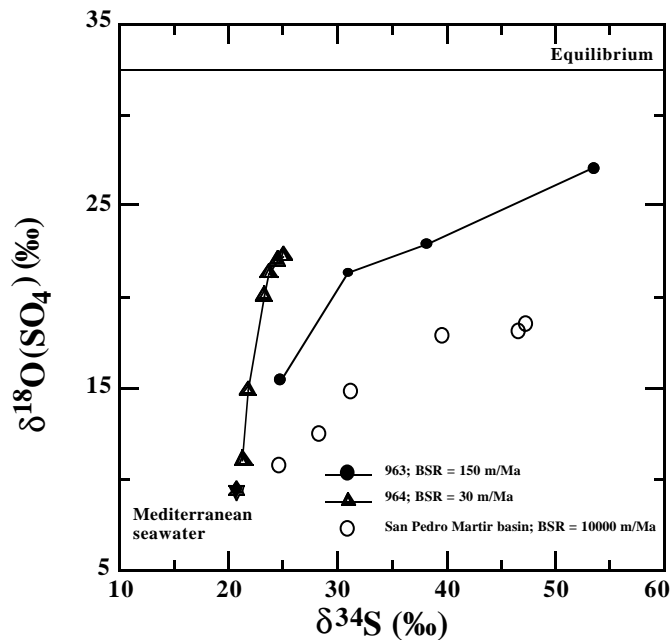


Figure 9. $\delta^{34}\text{S}$ vs. $\delta^{18}\text{O}$ values of residual sulfate of Sites 963 and 964 compared to pore waters from the San Pedro Martir basin, Gulf of California (Zak et al., 1980; bulk sedimentation rate (BSR) from Crusius et al., 1996).

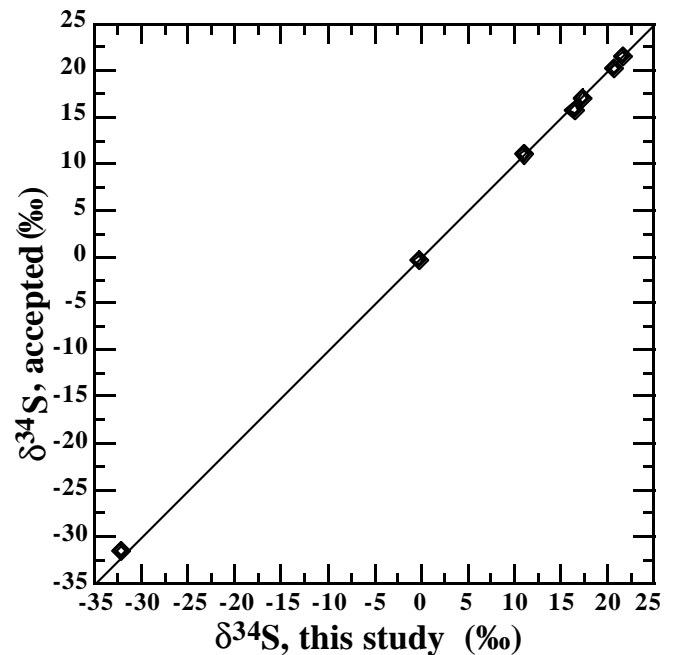


Figure 10. $\delta^{34}\text{S}$ values of IAEA intercomparison distributes and a synthetic CdS standard measured by the C-irmMS method of this study compared to the presently accepted values.